

Dynamics of ice forces on booms

Brian Morse

Cité Universitaire, Université Laval, Sainte Foy, Québec, Canada G1K 7P4

Received 12 October 2000; accepted 12 March 2001

Abstract

This paper presents the results of measured ice forces on three booms along the St. Lawrence River downstream of Montreal. We analyse (i) structural rupture events of various members, (ii) 44 recorded peak load events at 10 sites and (iii) 22 time series at five sites occurring over a 6-year period. The three booms (totalling 5 km in length), consist primarily of 61-cm diameter cylindrical pontoons. Time series data show that, during the consolidation period as the ice grows in area, thickness and strength, the load on the booms rise to a peak. Event analyses show that peak loads during a mid-winter thaw or during spring break-up are usually less severe. Fourier analyses show that the flexibility of the ice boom structure filters out high frequency loads. Even though most annual peak loads correspond to the theoretical value of the boom's normal retention capacity (5 kN/m), they often correspond to theoretical peak values possible during non-stable boundary conditions (10 to 15 kN/m). Finally, we propose formulae to assess the annual risk of exceeding a load value as a function of boom length. © 2001 Elsevier Science B.V. All rights reserved.

Keywords: Ice booms; Ice forces on structures; Cylindrical pontoons; St. Lawrence River

1. Introduction

The *Ice Engineering Manual* of the US Corps of Engineers (Ray, 1982) presents design and measured loads for various flexible ice boom geometries. For the standard Douglas Fir rectangular wooden booms, peak measured line loads vary from 6.7 to 10.7 kN/m; typical design values reach 16 kN/m. The recorded maximum for the huge rectangular steel boom at Beauharnois, Quebec, is 46.7 kN/m. For the 1996–1997 season, Cowper et al. (1997) report a peak line load of 14.1 kN/m on the 76-cm steel pontoon Lake Erie boom and a maximum tension of 330 kN in the chain connecting the monitored pon-

toon to the section cable. Cornett et al. (1997, 1998) report maximum observed loads (10 kN/m) for three seasons at some St. Lawrence River booms constructed of cylindrical steel pontoon (Fig. 1). They include a simple force balance analysis and statistical analysis based on peak daily values. Unfortunately, the daily peak values are not independent and therefore the statistical analyses only indicate associated probabilities. In this paper, we include 3 years of additional data, analyse complementary measurements not available to Cornett et al., perform a semi-dynamic force balance analysis and a statistical analysis of temporal independent maxima.

The data stems from three original deployment sites of a unique ice boom. The sites are on the St. Lawrence River, 40, 50 and 100 km downstream of

E-mail address: Brian.Morse@gci.ulaval.ca (B. Morse).

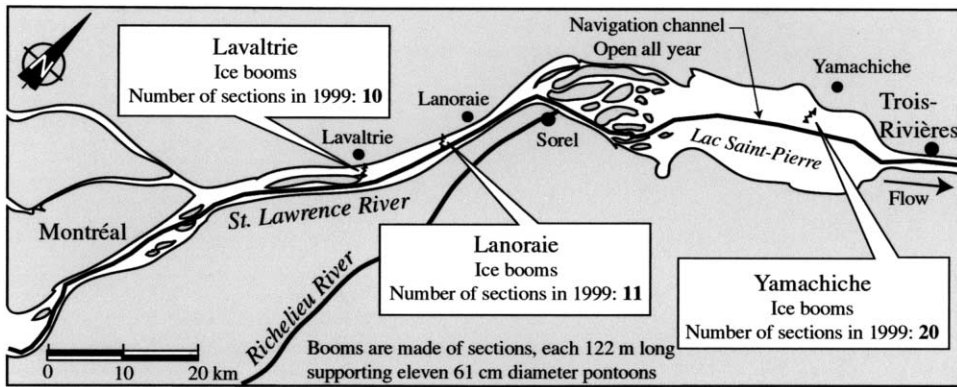


Fig. 1. Location map of St. Lawrence River ice booms downstream of Montréal, Canada.

Montréal, known, respectively, as the booms at Lavaltrie, Lanoraie and Yamachiche.

2. Boom description

To minimise risks of ice jams in the navigation channel downstream of the Port of Montreal, in 1993, the author (at the time, an employee of the Canadian Coast Guard) designed and deployed a new type of ice boom. Whereas most booms were previously made of rectangular (36 by 56 cm) sections of Douglas Fir, the new booms were cylindrical steel pontoons 61 to 76 cm in diameter and 914-cm long. Since then, the US and Canada deployed a number of these new cylindrical booms.¹

Yamachiche was the first cylindrical pontoon structure to be deployed on the St. Lawrence River. The first test of the cylindrical design used a single span in 1993. 1994 saw the first full deployment consisting of 19 sections, each 112-m long and consisting of 13 cylindrical pontoons. Most pontoons were 61 cm in diameter. In three of the sections, pontoons were 76 cm in diameter. The following year (1995), we removed all 76-cm pontoons and removed two pontoons from each of the remaining

sections (to allow more spacing between pontoons and therefore less banging into each other during wave events). The following year, a section was added at the south end to promote ice bridging between the boom and a nearby artificial island (known as “island no. 4”).

The Lavaltrie boom had eight sections, each consisting of 13 rectangular wooden pontoons. From 1993 to 1995, we added two more sections and replaced the 13 wooden pontoons with 11 cylindrical steel pontoons, 30% of which were 76 cm in diameter and 70% of which were 61 cm. The two additional sections enclosed that part of the channel that had eroded since the initial boom deployment in 1966.

The Lanoraie boom, 10 km downstream of Lavaltrie, was initially a 9 section—13 wooden pontoon structure, but in 1998–1999 became an 11 section—11 cylindrical 61-cm pontoon structure.

3. Ice formation

Both the Lavaltrie and the Lanoraie booms were typical installations, positioned at the downstream end of very elongated islands forming a secondary channel of the north bank of the St. Lawrence River (Fig. 1). Ice growth at Lavaltrie began as a triangle of loose floes behind the booms that originated upstream of Montréal. When additional ice floes met the triangle, they simply moved around each end of the boom, often entrapped by the Lanoraie boom located 10 km downstream. As border ice grew

¹ At each site, the diameter may have varied slightly, but the overall design remained the same. Sites include Lake Erie (for the New York Power Authority), the Rideau River (for the City of Ottawa), the Ottawa River (for the local hydropower station) and the forebay of Pickering nuclear power plant.

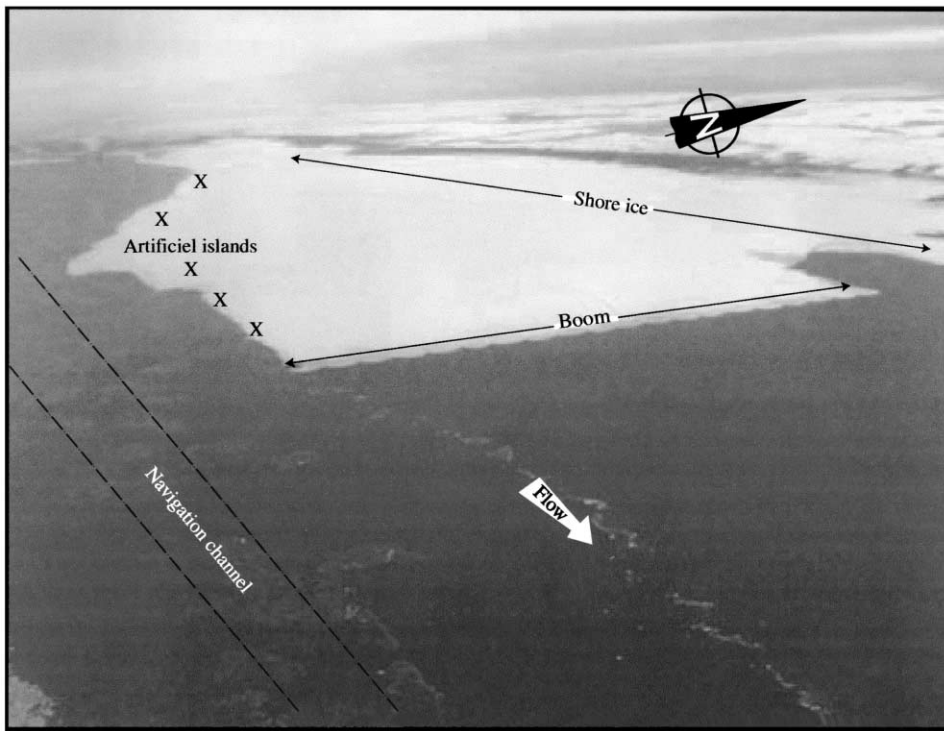


Fig. 2. Yamachiche boom on Lac Saint-Pierre with a fully developed ice cover upstream of it.

along the north bank of the river and along the islands on the south side of the channel, the upstream floes bridged the gaps and the whole channel began to form its cover. Prior to converting to the new cylindrical pontoons, there were many winters when no stable ice cover formed at Lavaltrie. In comparison, the new cylindrical boom design succeeded in forming a stable ice cover every year since its inception.

Whereas the two booms at Lavaltrie and Lanoraie promoted an ice cover that is eventually well confined between two parallel banks, the ice confinement at Yamachiche was a little more complex. At Yamachiche, the left side of the area upstream of the boom is the north side of Lake St. Pierre. On this side, very early on, extensive border ice formed and was well frozen into the bank. When the cover formed behind the boom, it immediately froze to this border ice. On the right (south) side, there was the 12-m deep navigation channel operating 365 days a year. Therefore, a series of artificial islands and navigation lights prevented the ice sheet from break-

ing away from the north area behind the boom and drifting into the navigation channel. The cover, formed in the area upstream of the boom, eventually froze into these islands after many weeks. The cover therefore was bound on the north side as border ice right from the beginning and on the south side only eventually bound onto the artificial islands (Fig. 2). The upstream end of the subject area (20 km upstream of the boom) is the Sorel Delta, which froze early in the season. Therefore, most incoming ice to the boom consisted of large sheets of thin (2–6 cm) columnar ice (“nilas”) generated locally.

4. Environmental forces

At Lavaltrie and Lanoraie, the ice cover area upstream of the boom had a triangular shape until the ice arched from the boom to the bank between the shore and an elongated island (Morse, 2001). The local depth (H) was about 4.5 m. Arching can cause

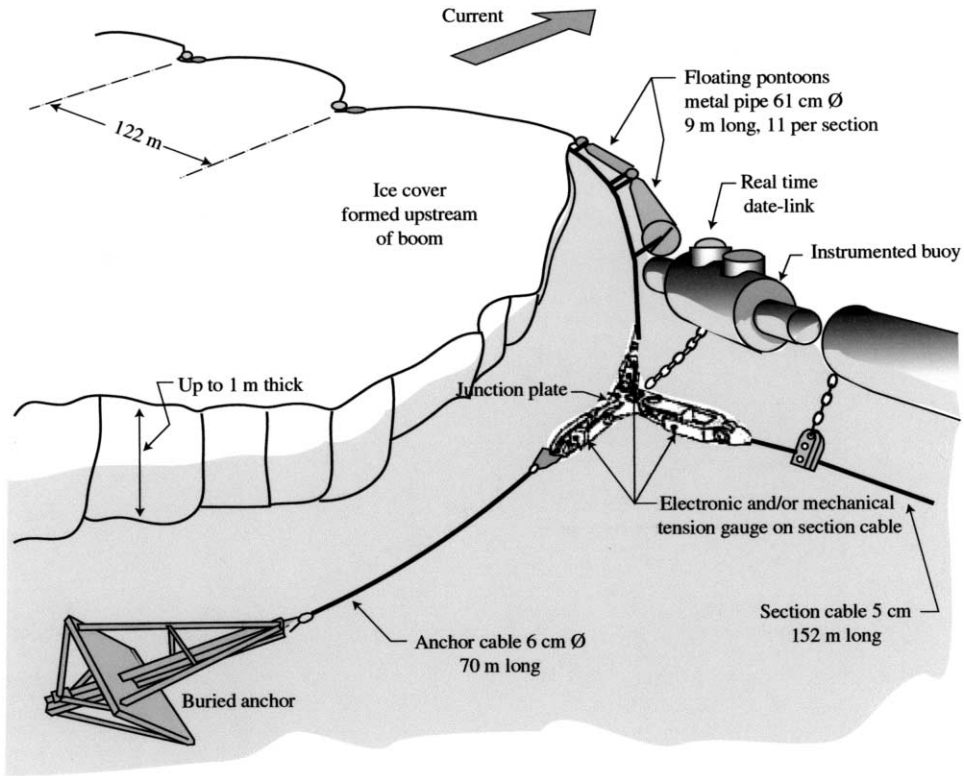


Fig. 3. Typical ice boom assembly showing load cells for force measurement.

the contributing area to jump from $0.3W^2$ to $3W^2$. The literature indicates that the water drag coefficient can also vary by an order of magnitude (from 0.005 to 0.05). Given a channel width $W = 1400$ m, a water density of a 1 mg/m^3 and an approximate water velocity of $V = 0.5 \text{ m/s}$, the environmental line load can easily vary from $f_w = 0.005 (1) (0.3 \times 1400^2) (0.5)/1400 = 0.5 \text{ kN/m}$ to $f_w = 0.05 (1) (3 \times 1400^2) (0.5)/1400 = 50 \text{ kN/m}$ depending on the value of the drag coefficient and the effective area.

In addition to the water shear on the ice cover, winds as much as 20 m/s can develop. Using a wind drag coefficient corresponding to rafted ice (0.003) and an air density of 0.0013 mg/m^3 , the wind line load can vary from zero (no wind condition) to $f_a = 0.003 (0.0013) (3 \times 1400^2) (20^2)/1400 = \pm 7 \text{ kN/m}$. Therefore, at Lavaltrie and Lanoraie, one could have expected the environmental line load to vary anywhere from $f_i = 0$ to 60 kN/m . Noting at

Yamachiche that $W = 2800 \text{ m}$, $H = 3 \text{ m}$, $V = 0.3 \text{ m/s}$, $f_w = 0.4$ to 40 kN/m and f_a can reach $\pm 14 \text{ kN/m}$. The total line load can therefore vary between $f_i = 0$ to 54 kN/m . Given the imprecision in the parameters, the value of 50 kN/m is used to represent potential maximum loading condition at all three sites. Because they contribute little in comparison with the wind and water shear forces, we ignore other environmental forces² such as the weight component of the ice sheet, the hydrostatic pressure at the upstream end and thermal expansion (Carter, 1994).

² It would be interesting to try to document and model the actual time series of environmental forces and compare them to measured loads. However, to date, we have not had the resources to undertake such a venture and we can therefore only offer the range in values as a backdrop to the observed loads presented in the next sections.

5. Applied line loads based on breakages

One way to determine ice/structure interaction, i.e. ice loads on structures, is to examine breakage events. While Douglas Fir pontoons occasionally broke in half, the new steel cylindrical pontoons have never shown signs of failure.

There was a 1.2-m chain at each end of each of the 11 pontoons to connect them to the section cable (Fig. 3). Normally, the chains break at a load of 220 kN (although we have, in some instances, used stronger chains). Every year, on average, three to four chains break. This is equivalent to a local “line load” in excess of $220 \text{ kN} \times 2 \text{ chains/pontoon} \times 11 \text{ pontoons/section cable} / 122 \text{ m/section cable} = 40 \text{ kN/m}$.

Each section consisted of a set of 11 pontoons and spans 122 m by a section cable 152-m long that sagged 41 m. At the junction with the anchor cable, the section cable’s corresponding angle, perpendicular to the flow, was $\alpha_4 = 53.4^\circ$ (Fig. 4). The section cables were “6/19 wire ropes” having an ultimate strength of 1500 kN. These section cables have broken at times. However, it was difficult to estimate the associated line load because at the time of the breakages, the cables were old and fatigued. No new section cables have ever broken. We can therefore infer that line loads averaged over a whole section did not exceed $1500 \text{ kN} \times 2\sin(53.4^\circ) / 122 \text{ m} = 19.7 \text{ kN/m}$.

Recently, 700-kN mechanical fuses have been inserted in series with the section cables to address a design flaw in the sizing of the anchor cables at Lavaltrie. In both 1999 and 2000, fuses broke where the boom had frozen into shallow fast ice. This indicates a line load in excess of 16 kN/m. In one of the events, the junction plate also tore apart; however, we made no structural evaluation of the associated force.

Anchor cables held the section cables. Given the section cable geometry, these normally carried 1.6 times the load of section cables ($2\sin(53.4^\circ)$). Prior to inserting the fuses in 1994–1995, a number of cables broke at Lavaltrie (Abdelnour et al., 1993). However, it was difficult to estimate the causative line load because they were old cables. Assuming they were at 75% of their 1500-kN strength, the causative line load could have been $1500 \text{ kN} \times 75\% / 122 \text{ m} = 9 \text{ kN/m}$.

Anchors have been known to migrate a little downstream in the first year following deployment. However, no anchor breakages have occurred on the St. Lawrence booms.

6. Measured line loads

We installed two types of measurement gauges, contained in the same cage, on both the St. Lawrence

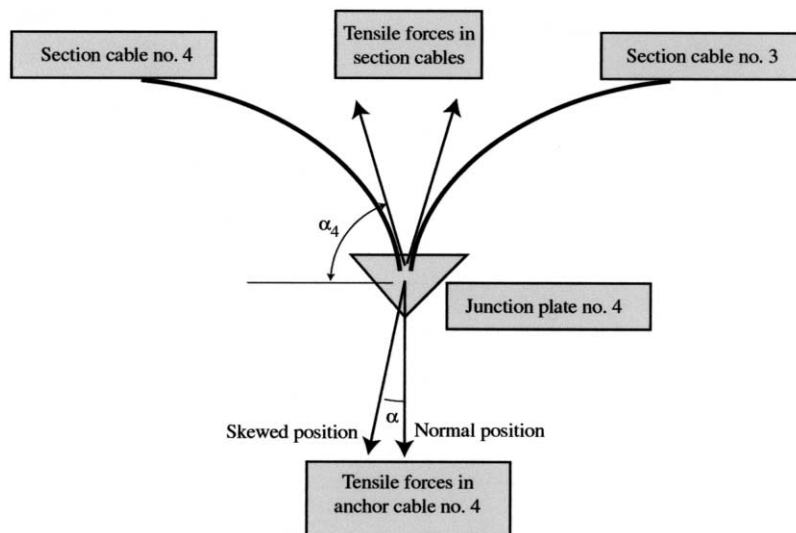


Fig. 4. Force balance at junction plate joining section cables to anchor cable.

ice booms section cables and anchor cables. These gauges worked in compression and therefore the cage translated cable tension into compression. The first gauge was a traditional load cell, hooked up to a real-time data acquisition system (Morse and Crookshank, 1998). The system sampled the loads twice a second and stored the instantaneous and maximum values of each 2-min period in a data file. In addition, it stored the local 2-min maximum and hourly maximum in a second data file and the daily maximum in a third data file.

The second measurement gauge consisted of three steel ball bearings about 1 cm in diameter placed between two aluminium plates about 1.5-cm thick by $10 \times 10 \text{ cm}^2$. After removing the booms from the river at the end of the season, the maximum load at each sampled location were calculated using a method similar to the Brinell hardness test. Depending on how great the maximum load was, the ball bearings imprinted themselves more or less into the plates. In the laboratory, the proportionality between the ultimate load and the depth of the penetration was established through cyclical loading of the ball bearing sandwich. Based on load cell measurements in the field, we then adjusted the calibration curve by -8% to account for the longer duration of the applied loads in the field. Except for one value at

Lavaltrie during 1998–1999, the agreement between the two measurement methods was excellent (Fig. 5). We believe that the discrepancy of that one event was caused by a malfunction of the local cell at the time.

In summary, we have two data sets. First, load cells provided the time series data. At Yamachiche, we deployed loads cells on all cables at junction plate locations nos. “4, 9 and 14” (Fig. 6). At Lanoraie and Lavaltrie, we monitored anchor cables (only) at one location mid-way along each of the booms.

The second data set consisted of the ultimate annual load recorded by mechanical means using the ball bearing sandwiches. We installed these gauges not only at all load cell locations but at many other locations as well. At Yamachiche, we also installed them on anchor cables nos. “1-south, 1-north, 3, 7, 13, 17 and 18” in addition to those installed on the anchor and section cables at junction plates nos. “4, 9 and 14”.

6.1. Inter-annual and spatially variable peak load values

Table 1 presents our best estimate of the peak annual loads at each of the gauged locations. A

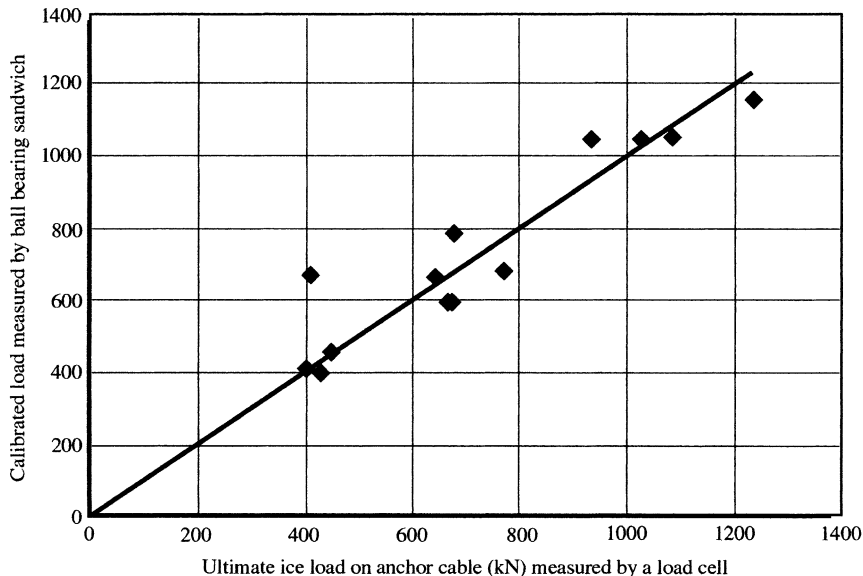


Fig. 5. Comparison of peak annual loads as measured by mechanical means and by load cells.

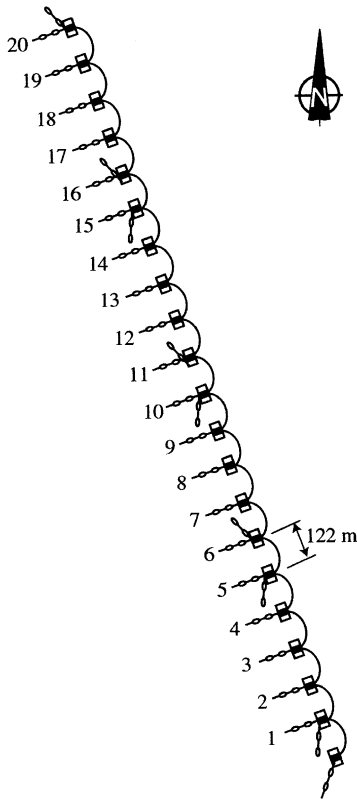


Fig. 6. Layout of Yamachiche boom.

combination of both data sets formed these data. Fig. 7 is a graphical presentation of data for the Ya-

machiche boom only. The load at anchor no. 17 during 1998–1999 really stands out. We believe that the mechanism causing this high value was very different from the norm. We believe it was a product of an ice management break-up strategy initiated by the Canadian Coast Guard using its hovercraft. The second striking characteristic of Fig. 7 is that there seems to be no discernible pattern to the loads. In other words, despite our expectations to the contrary, we do not find higher loads in the center of the boom, nor do we find higher loads on the south side (A3 and A4) as compared to the north side (A17 and A18).

The ultimate line loads vary by a factor of 5 (between 3 and 15 kN/m). In general, we can see that the winters 1995–1996, 1996–1997 and 1999–2000 are years with higher loads while the winters of 1997–1998 and 1998–1999 are lower than normal. We do not see a grouping of forces (A3 and A4, A7 and A9, etc.) that one would expect (because of their relative proximity and the boom’s ability to redistribute locally high loads) although it seems that there is less variation in loads across the boom that there is between years. However, there are insufficient data points in space and time to statistically show any significant spatial or temporal dependence. So until we amass several more years of data, we will necessarily treat the values as quasi-independent—knowing full well that there are certainly some interdependencies.

Table 1

Maximum peak annual line loads (kN/m)

Peak annual line loads (best estimate using data from load cells and mechanical means).

| | Anchor location | | | | | | | | | | |
|------------------------|-----------------|----------|----------|------|------------|-----|------|-----|------|-------|-----|
| | Lavaltrie | | Lanoraie | | Yamachiche | | | | | | |
| | mid boom | mid boom | 3 | 4 | 7 | 9 | 13 | 14 | 17 | 18/19 | A19 |
| 1994–1995 ^a | 6.2 | 2.8 | 5.9 | | 5.9 | | 7.8 | | 4.1 | 7.6 | |
| 1995–1996 | 5.5 | 5.5 | 10.9 | | 8.6 | | 6.3 | | 7.5 | 7.1 | |
| 1996–1997 | 8.6 | 5.1 | 9.9 | 6.2 | 10.6 | 8.9 | 10.9 | 8.6 | 5.9 | 9.3 | |
| 1997–1998 | 6.4 | 5.5 | 8.0 | 3.5 | 4.1 | 3.7 | 5.6 | 3.4 | 5.3 | 3.8 | |
| 1998–1999 | 5.5 | 3.5 | 2.9 | 6.6 | 2.9 | 3.7 | 6.1 | 5.6 | 14.8 | 6.5 | |
| 1999–2000 | 7.0 | 5.1 | | 10.6 | | 8.9 | | 6.4 | | | |
| Mean value | 6.5 | 4.6 | 7.5 | 6.7 | 6.4 | 6.3 | 7.3 | 6.0 | 7.5 | 6.7 | 7.6 |
| Maximum value | 8.6 | 5.5 | 10.9 | 10.6 | 10.6 | 8.9 | 10.9 | 8.6 | 14.8 | 9.3 | 7.6 |

^aActual locations of measured loads during 1994–1995 are uncertain.

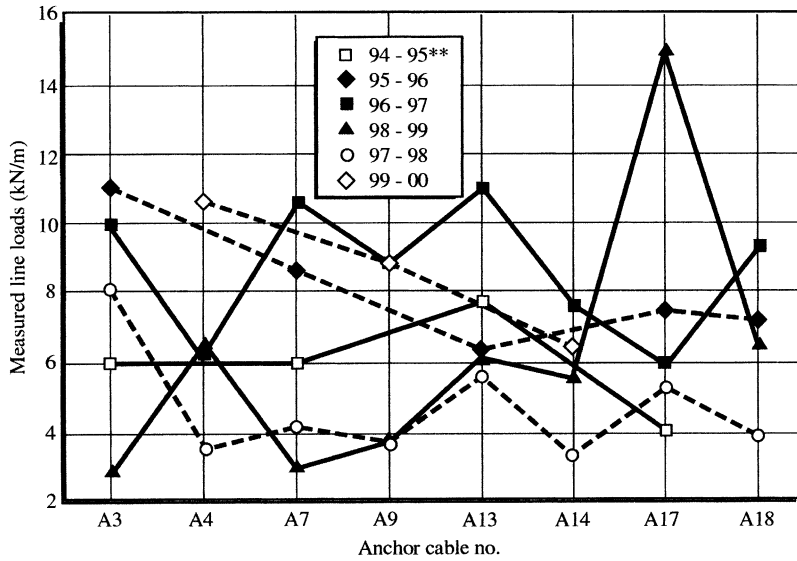


Fig. 7. Peak annual line loads at Yamachiche.

6.2. Seasonal load fluctuations

Fig. 8 presents the 2-min instantaneous measured loads in the anchor cable at junction plate no. 4 of

the Yamachiche ice boom. Fig. 8 is one of the 22 analyzed time series and, due to space considerations, is the only one specifically presented here in detail. An examination of all available series shows

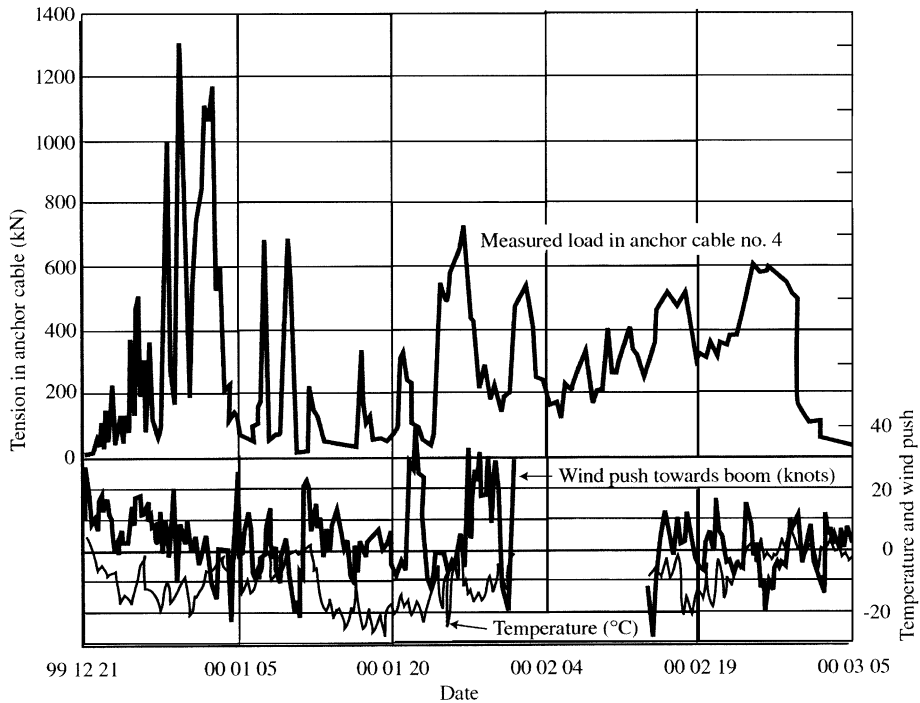


Fig. 8. Load on Yamachiche boom, Lac Saint-Pierre at junction no. 4.

that all share some similar characteristics. First, there is the period during which the ice cover consolidates and thickens. As the ice area upstream of the boom grows, environmental loads increase. As the ice thickens, more of the environmental load passes on to the boom. For the chosen example, the load increases from December 21st, 1999 to a maximum of 1275 kN (10.4 kN/m) on the 30th. Subsequently, as the ice sheet froze into the northern bank and into the artificial islands to the south, forces on the boom gradually diminished to near zero on January 6th, 2000. During some years, the mid-winter load drops to zero and stays there for several months. However, the 1999–2000 winter was very mild and there were many mid-winter events during January. We associate the maximum “mid-winter” event to the 707 kN load (5.8 kN/m), which occurred on the 26th of January. This mid-winter event may be partially caused by a 2-day storm during which time winds topped than 40 knots in a downstream direction. “Break-up” seems to begin in early February and forces reach a maximum 585 kN (4.8 kN/m) on February 24th. By February 29th, all the ice cover was gone.

For each of the 22 time series, we performed the same type of analysis. We identified a consolidation period, a winter period (which may or may not have mid-winter events) and a break-up period. Typically, the consolidation period lasted 2 to 4 weeks, the winter period 2 months and the break-up period 1 to 2 weeks.

The resulting data (Table 2) show that during any given year at any location, the peak annual load can occur during any of the three seasons. Nevertheless, the consolidation period normally generates the largest loads. On average, loads generated during break-up represent 65% of those during freeze-up. Mid-winter events, though sometimes severe, are, on average, only 50% as those generated during the consolidation period.

7. Spectral analysis

Fig. 9 presents the results of a Fourier analysis of the 2-min values displayed in Fig. 8. Clearly, most of the energy corresponds to a 28-day period. This

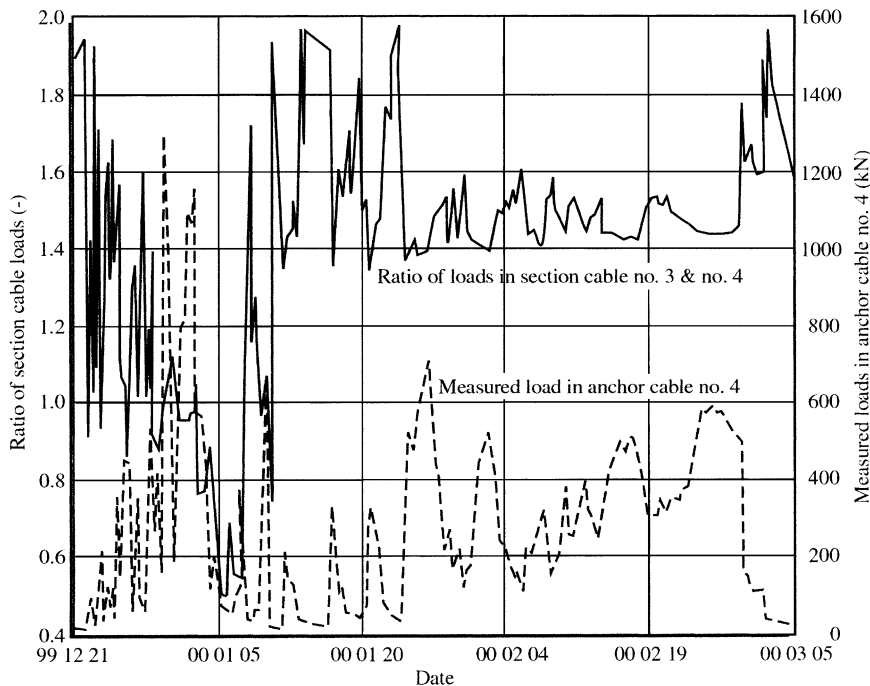


Fig. 9. Ratio of loads in section cables at anchor plate no. 4.

indicates that the most important dynamic is the consolidation period. Interestingly, there are also energy peaks at 14 and 7 days that lead us to wonder if there is a link with the lunar periodicity of the small (15 cm) tide in the area. Despite the fact that the anchor cable load can vary from 50 to 1200 kN within any single day during December, the spectral analysis shows that there is comparatively little energy in events lasting 1 day or less when compared to the energy in the longer loading cycles. This is an important finding from a design point of view. It means that the boom is truly a very flexible structure that absorbs and redistributes impact loads (Timco and Cornett, 1996).

7.1. Lateral force dynamics

A force balance analysis shows that the load in one cable influences the load on all other cables. In fact, in a perfectly symmetrical boom having equal section spans, the force in all section cables should be equal. However, as Fig. 9 demonstrates, the load in one section cable can be twice as much as the load in the other.

There are three elements that promote independence between loads in individual cables. At the Yamachiche boom, given that there are lateral anchor cables at junction plate nos. 1, 5, 6, 10, 11, 15 and 16, forces in section nos. 1 to 5, 5 to 10, 10 to 15, 15 to 19 and 0 (all by itself) can act as five independent sub-systems.³ Secondly, boom sections move laterally to absorb non-uniform loading. Hence, only a certain percentage of the load differential passes on from one section to its neighbour.⁴ Thirdly, the ice cover upstream of the boom absorbs within itself some of the non-uniform loading. When the ice aggregate is thick and dense or when the cover is consolidated, this internal mechanism may be a very effective filter of non-spatially homogenous forces.

Consider the situation shown in Fig. 4 when the force in one section cable (say no. 3) is greater than

that in an adjoining section cable (say no. 4). In order for the force balance to be preserved in the cables, the junction plate (no. 4) must move some amount X to the right. This implies that the span of section no. 4 increases by X and that of section no. 3 decreases by X . The geometric relationships applicable to parabolas can easily determine the new angles 3 and 4. There will also be a shift in the anchor cable alignment. If the length of the anchor cable is L then the angle shift will be very close to the value $\alpha = X/L$. Substituting these values into the force balance at the junction plate leads to the following equation where T_3 , T_4 , α_3 and α_4 are the tensions and angles in section cables no. 3 and no. 4, respectively:

$$\frac{T_3}{T_4} = \frac{\cos(\alpha_4) + \sin(\alpha_4)\tan(\alpha)}{\cos(\alpha_3) - \sin(\alpha_3)\tan(\alpha)}. \quad (1)$$

Using this relationship and the loads presented in Figs. 8 and 9, we calculate a shift of up to 8 m in the junction plate. During the consolidation period (December 21st to January 10th), forces in section cable no. 4 are greater than those in no. 3 as a result of the triangular unconsolidated nature of the cover upstream. Later on, forces increase in section no. 3 relative to section no. 4 because the cover on the north side is well anchored into the shore, while the artificial islands to the south only partially absorb the load.

8. Force balance in cables at junction plates

Referring to Eq. (1) and Fig. 3, for static equilibrium, it is easy to write a force balance equation for measured forces in the section and anchor cables at the junction plate. The only missing element is the ice force on the barrel holding up the junction plate. Once we account for the fact that the instrumented barrel is almost as big as a regular pontoon, our analyses show that there is always a very good agreement between the vector sum of measured loads at junction plates (within 5%). Despite the sudden cable movements indicated in Fig. 9, this finding indicates that unbalanced “dynamic events” are not significant in the design nor in the analysis of boom cables.

³ These lateral cables were included in the initial design to prevent failure of the whole structure and to protect it against fierce broadside attacks that are quite possible in windy conditions given the position of the booms in the lake.

⁴ The further along the boom, the less influence an event has on section cables.

8.1. Statistical analysis

We performed a statistical analysis on the peak annual loads presented in Table 2. We limited data inclusion to those data that were both independent and respected data homogeneity.⁵ We chose 44 data points for inclusion. The range in values was 2.9–14.8 kN/m. The average value was 6.8 kN/m and the standard deviation was 2.5 kN/m. The coefficient of variation was 0.5 and the skewness coefficient was 0.8.

We analyzed these data against Normal, Lognormal, Lognormal-3, Gumbel, Pearson-3, Log-Pearson-3 and Generalized Extreme Value distributions. Fig. 10 presents the fitted distributions and measured data (plotted according to Gringoten’s formula). All distributions passed a statistical acceptance test at the 95% confidence limit except the Normal distribution (Fig. 11). All the others are pretty well equivalent. Table 3 presents the resulting statistics. On average, the medium ultimate annual line load was $F_{L50} = 6.4$ kN/m, the 95% probability line load was $F_{L95} = 11.5$ kN/m and the 99% probability line load was $F_{L99} = 14.4$ kN/m. Note that F_{L50} was slightly lower than the calculated mean (6.8 kN/m). In addition, F_{L99} was slightly lower than maximum measured value $F_{Lmax} = 14.9$ kN/m. Given the goodness of fit of the distributions and the consistency of the results, these statistics were representative of the ice/structure interaction phenomena of these booms.

How can one generalize these results for booms located elsewhere? If we accept that the data really represent independent events equivalent to 44 winters then we can say that there is a 1% chance of having a line load in excess of 14.4 kN in any given year. However, we feel that (i) there must be some interdependence between measured values and (ii) the data are not representative of 44 years.

We could use our knowledge that the Lognormal distribution is representative of the process and analyse only the maximum peak loads regardless of location for each year (six data points). The resulting calculated line loads result in $F_{L50} = 10.3$, $F_{L95} =$

Table 2
Maximum peak seasonal load (kN)

| | | Consolidation period | Mid-winter period | Break-up period |
|-----------|-----------|----------------------|-------------------|-----------------|
| Lanoraie | 1994–1995 | 340 | | |
| | 1995–1996 | 667 | | |
| | 1996–1997 | | | |
| | 1997–1998 | 302 | 201 | 637 |
| | 1998–1999 | | | |
| Lavaltrie | 1999–2000 | 369 | 619 | 611 |
| | 1994–1995 | 751 | | |
| | 1995–1996 | 673 | 258 | 344 |
| | 1996–1997 | 1023 | 78 | 621 |
| | 1997–1998 | 661 | 59 | 675 |
| Yam-no.4 | 1998–1999 | 404 | 72 | 375 |
| | 1999–2000 | 850 | | 432 |
| | 1994–1995 | | | |
| | 1995–1996 | | | |
| | 1996–1997 | 762 | 237 | 437 |
| Yam-no.4 | 1997–1998 | 402 | 426 | 380 |
| | 1998–1999 | 333 | 801 | 382 |
| | 1999–2000 | 1297 | 707 | 585 |
| | 1994–1995 | | | |
| | 1995–1996 | | | |
| Yam-no.4 | 1996–1997 | 1084 | 198 | 765 |
| | 1997–1998 | 301 | | 447 |
| | 1998–1999 | 454 | 345 | 276 |
| | 1999–2000 | 1084 | 461 | 372 |
| | 1994–1995 | | | |
| Yam-no.4 | 1995–1996 | | | |
| | 1996–1997 | 932 | 117 | 344 |
| | 1997–1998 | 355 | 10 | 403 |
| | 1998–1999 | 684 | 507 | 519 |
| | 1999–2000 | 781 | 250 | 227 |

15.2 and $F_{L99} = 17.9$ kN/m. These statistics represent the maximum peak load likely to occur at any spot on any of the lower St. Lawrence River booms during any given year.

A more general method (for any boom built of 61-cm pontoons) would be to use the concept of risk. On average, we gauged about 7.3 locations each year during 6 years for a total of 44 events. Therefore, we can say that the actual risk R of not exceeding the given line load at any of the m gauged locations is:

$$R = P^m \tag{2}$$

where P is the calculated cumulative probability during the 44-event analysis and m is the number of quasi-independent locations that ice loads can be applied on a boom. In our application to the St.

⁵ Data homogeneity was not perfect because each boom installations was adjusted slightly each year.

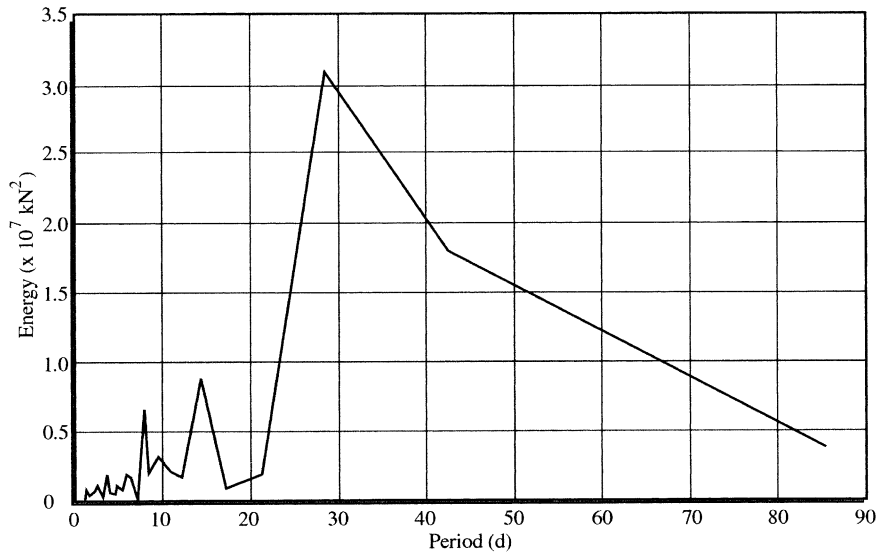


Fig. 10. Spectral analysis of 1999–2000 loads on anchor cable no. 4 at Yamachiche boom.

Lawrence booms, the line loads of 6.4, 11.5 and 14.4 kN/m were associated with the probabilities $P = 50\%$, 95% and 99% . The revised probabilities for these values (using the concept of risk expressed in Eq. (2)) would be $R = 1\%$, 69% and 93% . Therefore, we can say that for the St. Lawrence booms the data show that $F_{L01} = 6.4$, $F_{L69} = 11.5$ and $F_{L93} = 14.4$ kN/m. In other words, there is a 7% chance that the peak observed line load at any location on

any St. Lawrence boom during any given year would be greater than 14.4 kN/m.

To use this information for booms (of the same type and the same size) deployed elsewhere (in winter conditions where the environmental forces are greater than the boom's capacity to retain them), one could estimate the number of independent locations (m) based on the length of the boom. In our analysis, the total boom length was about 4.8 km and we had 7.3 quasi-independent locations. So to transfer the data to other locations, the value of m could be estimated as boom length $m = (7.3/4.8) \times$ boom length or $m = 1.52 \times$ boom length expressed in km.

For example, for a river having a 61-cm diameter boom, 2 km in length, $m = 1.52 \times 2 = 3.04$. Therefore, the probability of generating line loads less than or equal to 6.4, 11.5 and 14.4 kN/m in any given year would be $0.5^{3.04}$, $0.95^{3.04}$, $0.99^{3.04}$ corresponding to 12%, 86% and 97%, respectively.

Table 3
Results of statistical analysis of annual peak line load data

| Distribution | Estimated line load (kN) as a function of cumulative probability | | |
|---|--|-------|-------|
| | 50% | 95% | 99% |
| Normal | 6.79 | 10.96 | 12.69 |
| Lognormal | 6.34 | 11.85 | 15.35 |
| Lognormal-3 | 6.60 | 11.16 | 13.40 |
| Pearson-3 | 6.46 | 11.44 | 14.11 |
| Log-Pearson-3 | 6.43 | 11.57 | 14.46 |
| Gumbel | 6.36 | 11.67 | 14.99 |
| Generalised extreme value | 6.46 | 11.50 | 14.24 |
| Average (not including the normal distribution) | 6.4 | 11.50 | 14.40 |

9. Key findings

9.1. Peak loads

- Peak annual loads at Lavaltrie were, on average, 8% lower than the average peak annual load at Yamachiche.

- Peak loads at the Lanoraie during the time of a rectangular timber boom deployment were 20% lower.

- Based on 44 monitoring sites covering 6 years of data at three booms comprised of 61-cm cylindrical pontoons and totaling 4.8 km in length, the average peak annual load was 6.4 kN/m. The maximum recorded line load was 14.4 kN/m but this load occurred due to Coast Guard ice-breaking activities. Otherwise, the maximum recorded line load was 10.9 kN/m. According to measurements and an analysis of ruptured structural elements, loads in excess of 9 kN/m were almost annual occurrences. No new section cable has ever broken suggesting that the maximum line load never exceeded 19.7 kN/m anywhere. On the other hand, annual chain failures testified to very localized line loads in excess of 40 kN/m.

- With the exception of the Normal distribution, virtually all the statistical distributions (Lognormal, etc.) fit the peak annual load data extremely well (Fig. 11).

- For St. Lawrence booms, the probability of the peak load being less than or equal to 6.4, 11.5 and 14.4 kN/m at any particular gauged location is 50%, 95% and 99%, respectively.

- Since the St. Lawrence booms have seven gauged locations, the annual probability of the peak load being less than or equal to 6.4, 11.5 and 14.4 kN/m at any of the seven gauged location is 1%, 69% and 93%, respectively.

- For deployments elsewhere of 61-cm cylindrical pontoons, in winter conditions similar to those of the Montreal area, on rivers where environmental loading exceeds boom resistance, the probability of the structure receiving line loads less than or equal to 6.4, 11.5 and 14.4 kN/m at any location is 0.50^m , 0.95^m and 0.99^m , respectively, where $m = 1.52$ times the length of the boom (expressed in km). In addition, these values may be fitted to one of the theoretical distributions (Lognormal, etc.) to extrapolate or interpolate values for any other return period.

- These statistics should be interpreted against the backdrop of physical processes. We recall that the type of ice accumulation upstream of the St. Lawrence booms is best represented as an ice sheet and not as ice rubble. Secondly, we assume that the line load on the structure at any given time will be the least of either (i) the environmental driving force which pushes the ice against the boom, (ii) the internal resistance of the ice sheet (it must have sufficient internal strength to transmit forces to the

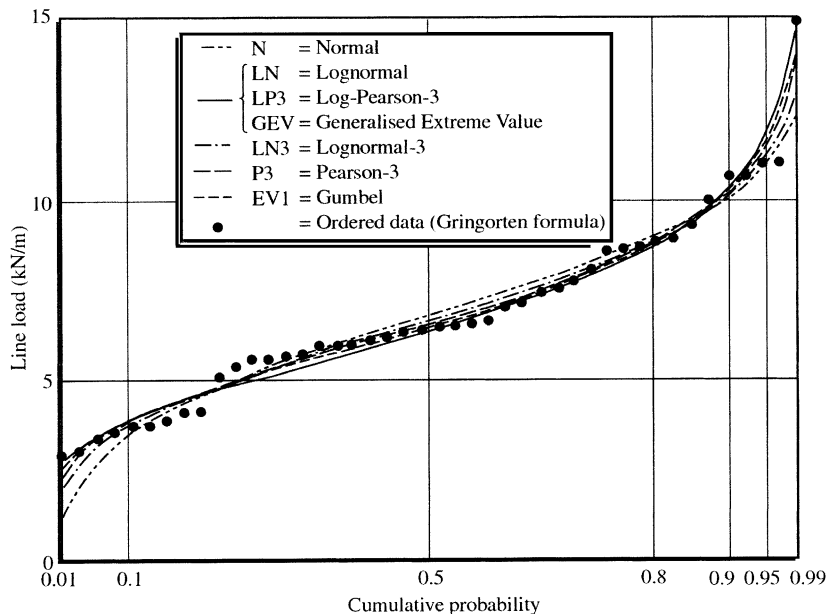


Fig. 11. Statistical distributions of annual peak line loads.

boom) and (iii) the boom's theoretical ability to resist that push (before it is submerged by the force of the ice sheet):

- With regards to the environmental push, under extreme conditions, one could expect a water drag force of 40 kN/m at Lavaltrie and Lanoraie and 30 kN/m at Yamachiche. Wind drag can add or subtract (depending on wind direction) an additional 10 and 15 kN/m, respectively. At other times, a lower drag coefficient and/or a smaller contributing area can reduce line loads by a factor of 100. Of course when the line loads reach extreme values, the push is beyond the internal resistance of the ice sheet and/or the boom's capacity, resulting in an ice run.
- (ii) For consolidated ice sheets greater than 30-cm thick, the ice is competent enough to transmit the forces without internal failure
- (iii) The capacity of the boom to retain ice is highly dependent on the ice thickness, on the ice/pontoon interface boundary conditions and on the value of the coefficient of friction μ between the ice and the pontoon. Measured loads (4 to 15 kN/m) are consistent with a theoretical estimate of the boom's capacity.

9.2. Spatial–temporal analysis

- The flexibility of the boom structure tends to redistribute local loads. The exceptions (by observed structural failure) are those sections close to the riverbanks. At times, these sections can be subject to very high local forces generated by booms being frozen into the ice cover.

- There are not statistically discernable trends neither in the lateral nor inter-annual variation of line loads over the width of the structure.

- Section cable analyses show that the seasonal force in one cable can be up to two times the force in the neighbouring section cable. The boom adjusts to the non-uniform loading by modifying its span lengths. The calculated junction plate movement is about 8 m for the Yamachiche boom.

- Field data and theoretical analyses tend to show that maximum loads at one anchor cable are more or less interdependent of those in its neighbours. We

prefer using the assumption that the nearest neighbours are dependent while those further away are virtually independent. However, because of the slight interdependence of the loads, our statistical analyses have a small bias that results in a slight underprediction of the line load statistics.

9.3. Loading dynamics

- Maximum 2-min loads are about 3% greater than loads sampled at 2 Hz.
- Maximum hourly loads are about 3% greater than maximum 2-min values.
- During the consolidation period, loads may substantially vary during the course of any given day (from 50 to 1000 kN).
- Spectral analysis shows a logarithmic decline of energy with increasing frequency.
- Spectral analysis shows that there seems to be peak loads every week and/or every other week. The overwhelming energy content corresponds to the length of the consolidation period. This normally last between 2 and 4 weeks.
- A seasonal analysis of the loading at many locations over the 6-year period shows that the peak annual load can happen during any given season. However, normally, it happens during the consolidation period, less often during break-up and even less often during a mid-winter event.
- On average, peak loads during the consolidation period are normally 40% higher than peak loads at break-up and 50% higher than peak loads during mid-winter events.

9.4. Design considerations

Our analysis shows that the 61-cm pontoon cylindrical ice boom is a very efficient structure. Due to its three-dimensional nature, the boom effectively filters out high frequency and eccentric loading. Flexibility in the structure appears to favour low dynamic load interactions with the ice sheet. Peak local loads are distributed and high-frequency impact loads are negligible.

Boom design must maintain a balance between structural members' sizes (Foltyn and Tuthill, 1996).

The many ruptures of anchor cables, junction plates, old section cables, fuses and chains suggests that the relative strength of each element must be well balanced with respect to neighbouring elements. Chains must resist local line loads in excess of 40 kN/m; however, over-designed chains may tend to tear the section cable fibres unless one modifies the clamps as was done by Fleet Technology for the Lake Erie boom. Anchor cables must be at least 1.8 times stronger than section cables to ensure that section cables always break before anchor cables do.

When properly designed, experience on the St. Lawrence with the cylindrical pontoon booms shows that they are cost efficient rugged structures that are very efficient in forming and stabilising ice sheets.

Acknowledgements

This study was funded in part by the Ice/Structure Interaction Committee of the Panel on Energy Research and Development (under the management of Garry Timco) and by the National Science Engineering Research Council. We further wish to acknowledge our debt to previous researchers who aided in the design of the boom, especially Razek Abdelnour (Fleet Technology), Ed Stander, Donald Carter (Donal Carter and associates) and Andrew Cornett, Robert Frederking, Garry Timco (Canadian Hydraulics Centre). We also appreciate the collaboration of Gervais Bouchard, engineer of the Canadian Coast Guard (CCG). We thank Stéphane Dumont, the CCG engineer for overseeing the installation of the gauges and their calibration in addition to retrieving the data and creating the database. We thank Marc Choquette and Marc Savard also of the CCG team who were collectively responsible for monitoring and maintaining the booms and recording

instruments. We thank Ed Stander and James O'Regan for their comments and editorial review and those unknown reviewers of the manuscript version.

References

- Abdelnour, R., Gong, Y., Comfort, G., McGoey, L., 1993. Lavaltrie ice boom: preliminary design for new boom pontoons. Fleet Technology Report FTL-4319, Kanata, Ont.
- Carter, D., 1994. Forces sur les estacades. Report prepared for Transport Canada, Québec, Qué.
- Cornett, A.M., Frederking, R., Morse, B., Dumont, S., 1997. Ice boom loads in the St. Lawrence river, 1994–95 and 1995–96. Procs. 7th International Offshore and Polar Engineering Conference, ISOPE'97, Honolulu, USA, vol. II, pp. 442–448.
- Cornett, A.M., Frederking, R., Morse, B., Dumont, S., 1998. Review of ice boom loads in the St. Lawrence river, 1994–1997. In: Shen (Ed.), Ice in Surface Waters. Balkeman, Rotterdam, pp. 53–59.
- Cowper, B., Abdelnour, R., Yuxiang, G., Crissman, R., 1997. Ice load measurements on the Lake Erie–Niagara River Ice boom: 1996/97. 9th Workshop on River Ice, Fredericton, NB, Canada. Canadian Committee on River Ice Processes and the Environment, Fredericton, N.B., Canada.
- Foltyn, E.P., Tuthill, A.M., 1996. Design of Ice Booms. Cold Regions Technical Digest No. 96-1, April 1996.
- Morse, B., 2001. Ice: Booms or Bust—Theoretical development of ice forces on booms. Paper submitted to the ASCE J. of Cold Regions Engineering in October, 2000 and accepted for publication.
- Morse, B., Crookshank, N., 1998. The Canadian Coast Guard's environmental prediction decision support system—five years in the making. First International Conference on New Information Technologies for Decision Making in Civil Engineering, Montreal, Canada. École de technologie supérieure, Montréal, Canada, pp. 11–13, October.
- Ray, J., 1982. Department of the Army Corps of Engineers. Engineering Manual EM 1110-2-1612, Engineering and design, ice engineering. Office of the chief engineers, Washington, D.C.
- Timco, G.W., Cornett, A.M., 1996. Laboratory tests of ice interaction with steel booms. Canadian Journal of Civil Engineering, 23, 560–566.